Available online at www.sciencedirect.com
SCIENCE DIRECT
Biochimica et Biophysica Acta 1757 (2006) 781–786
BIOCHIMICA ET BIOPHYSICA ACTA
BBA
www.elsevier.com/locate/bbabio

Interaction between tyrosine$_Z$ and substrate water in active photosystem II

Chunxi Zhang *

Service de Bioénergétique, CNRS URA 2096, Département de Biologie Joliot-Curie, CEA Saclay, 91191 Gif-Sur-Yvette, Cedex, France
Laboratory of Photochemistry, Center for Molecular Sciences, Institute of Chemistry, Chinese Academy of Sciences, Beijing 100080, China

Received 31 December 2005; received in revised form 17 May 2006; accepted 18 May 2006
Available online 3 June 2006

Abstract

In the field of photosynthetic water oxidation it has been under debate whether Tyrosine$_Z$ (Tyr$_Z$) acts as a hydrogen or an electron acceptor from water. In the former concept, direct contact of Tyr$_Z$ with substrate water has been assumed. However, there is no direct evidence for the interaction between Tyr$_Z$ and substrate water in active Photosystem II (PSII), instead most experiments have been performed on inhibited PSII. Here, this problem is tackled in active PSII by combining low temperature EPR measurements and quantum chemistry calculations. EPR measurements observed that the maximum yield of Tyr$_Z$ oxidation at cryogenic temperature in the S_0 and S_1 states was around neutral pH and was essentially pH-independent. The yield of Tyr$_Z$ oxidation decreased at acidic and alkaline pH, with p*K*s at 4.7–4.9 and 7.7, respectively. The observed pH-dependent parts at low and high values of pH can be explained as due to sample inactivation, rather than active PSII. The reduction kinetics of $Tyr_Z^{\bullet}$ in the S_0 and S_1 states were pH independent at pH range from 4.5 to 8. Therefore, the change of the pH in bulk solution probably has no effect on the Tyr$_Z$ oxidation and $Tyr_Z^{\bullet}$ reduction at cryogenic temperature in the S_0 and S_1 states of the active PSII. Theoretical calculations indicate that Tyr$_Z$ becomes more difficult to oxidize when a H_2O molecule interacts directly with it. It is suggested that Tyr$_Z$ is probably located in a hydrophobic environment with no direct interaction with the substrate H_2O in active PSII. These results provide new insights on the function and mechanism of water oxidation in PSII.

Keywords: Photosystem II; Tyrosine Z; EPR; Substrate water; pH dependence; DFT calculation

1. Introduction

Photosynthetic oxygen evolution is a unique function of the Photosystem II (PSII) in cyanobacteria, algae and higher plants, which sustains most life in this planet. PSII is a multi-subunit membrane protein complex. The crystal structure of PSII is beginning to be clarified [1–4]. Upon excitation, the primary electron donor (P_{680}) donates one electron to the primary electron acceptor (Pheo) to produce the $P_{680}^{+\bullet}$ and $Pheo^{-\bullet}$ charge pair. $Pheo^{-\bullet}$ then transfers the electron to a quinone–iron complex in which the primary and secondary quinones (Q_A and Q_B) function in sequence. Meanwhile, $P_{680}^{+\bullet}$ drives the water oxidation in the catalytic center of the Mn-cluster containing four Mn ions, one Ca^{2+} and one or more Cl^- ions. The turnover of the Mn-cluster leading to water oxidation involves five different states (S_{0-4}), in which S_0 is the most reduced state, and S_1 is the dark stable state [5–8]. D_1-Tyr_{161} (Tyr$_Z$) is the secondary electron donor located between P_{680} and Mn-cluster in PSII.

An important question is how Tyr$_Z$ plays the role of tuning the one-electron photochemical reaction and the four-electron catalytic water oxidation process, thus controlling the water oxidation efficiently [9,10]. To answer this question, it is important to know the detailed protein environment of Tyr$_Z$ and its relationship with substrate water molecules and the Mn-cluster in active PSII.

Almost decade ago, Babcock and co-workers proposed a hydrogen–atom abstraction mechanism that Tyr$_Z$ tuned the water oxidation through direct interaction with substrate H_2O bound to Mn ions [11,12]. This model has been widely cited, and

Abbreviations: Chl, chlorophyll; DFT, density functional theory; DMSO, dimethyl sulfoxide; EPR, electron paramagnetic resonance; EDTA, ethylenediaminetetraacetic acid; HOMO, highest occupied molecular orbital; MES, 4-morpholine ethanesulfonic acid; MOPS, 3-morpholino propanesulfonic acid; P_{680}, primary electron donor of PSII; Pheo, pheophytin; PPBQ, phenyl-*p*-benzoquinone; PSII, photosystem II; Q_A and Q_B, primary and secondary quinone electron acceptors, respectively; Tyr$_Z$, tyrosine 161 of the D_1 protein; Tyr$_D$, tyrosine 160 of the D_2 protein

* Laboratory of Photochemistry, Center for Molecular Sciences, Institute of Chemistry, Chinese Academy of Sciences, Beijing 100080, China. Fax: +86 10 82617315.
E-mail address: chunxizhang@iccas.ac.cn.

0005-2728/$ - see front matter © 2006 Elsevier B.V. All rights reserved.
doi:10.1016/j.bbabio.2006.05.036

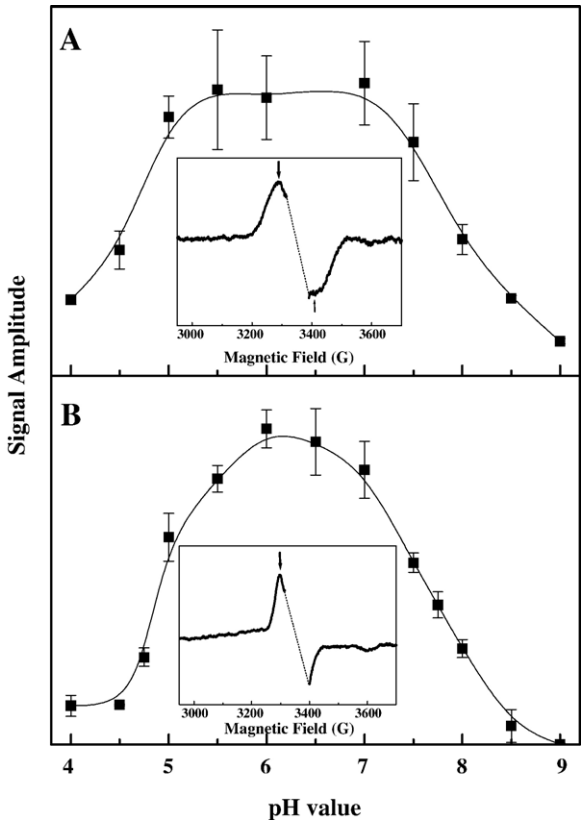

Fig. 1. pH dependence of the formation of the $S_0Tyr_Z^{\bullet}$ (A) and $S_1Tyr_Z^{\bullet}$ (B) signals. Each point is the average of the signal amplitude from three parallel samples. The amplitude of the $S_0Tyr_Z^{\bullet}$ was determined by using the difference absorption between peak and through marked in insert Fig. 1A. The amplitude of $S_1Tyr_Z^{\bullet}$ was determined by taking the absorption of the peak marked in insert Fig. 1B. Insert figure in A and B are $S_0Tyr_Z^{\bullet}$ and $S_1Tyr_Z^{\bullet}$ EPR signal induced from 0-flash and 3-flash PSII samples at pH 6.5, respectively. The region around $g=2.00$ corresponding to the $Tyr_D^{\bullet}$ signal is omitted. EPR conditions: temperature, 5 K; microwave frequency, 9.42 GHz; modulation frequency 100 kHz; microwave power, 25 mW; modulation amplitude, 25 G.

the idea of the direct interaction between Tyr_Z and substrate H_2O has been incorporated in many other models [13]. However, it should be pointed out that most evidences for this model were obtained from experiments on inhibited PSII samples (for example, Ca- [14,15], or Mn- [16–18] depleted PSII samples).

Recent PSII crystal structures [2–4] have revealed that Tyr_Z forms a hydrogen bond with D1-His190, which is consistent with most previous biochemistry studies [9,10]. However, the possible interaction between Tyr_Z and substrate H_2O is still far from an unambiguously demonstrated. Based on the 3.5 Å resolution data, Ferrira et al. [3] suggested that Tyr_Z interacted directly with a water molecule bound to Ca^{2+} (rather than a Mn ion) through a hydrogen bond, and that the water molecule further connected with a proton channel to the lumen. More recently, Yano et al. [19] have found that the oxidation state and the structure of the Mn-cluster, as well as, its ligand environments (especially, H_2O or OH^-, O^{2-}) may be significantly modified due to serious radiation damage rising from the X-rays during the crystal structure determination. Therefore, it is fair to say that current structural data provide only limited information on the possible interaction between Tyr_Z and substrate water molecule. On the other hand, spectroscopic studies on Tyr_Z in active PSII have been always suffered from its fast turnover and lack of spectroscopic characteristics [9,10]. However, most of our present knowledge on Tyr_Z came from investigations on inhibited PSII. However, it is well known that the properties of Tyr_Z in inhibited PSII can be dramatically different from that in active PSII [9,10]. For example, the Tyr_Z oxidation rate is thousand times slower in inhibited PSII than in active PSII [20,21]. It was suggested that Tyr_Z was located at a hydrophilic environment, and exposed to the bulk water in Mn-depletion PSII samples [9,10,22]. Therefore, it is necessary to verify directly if Tyr_Z does interact with substrate water in active PSII.

Recently, a relatively high yield oxidation of Tyr_Z in S_0 and S_1 states has been reported at cryogenic temperature in active PSII [23–27]. The magnetic interaction between $Tyr_Z^{\bullet}$ and S_0 or S_1 states of the Mn-cluster gives rise to two distinctive EPR signals attributed to $S_0Tyr_Z^{\bullet}$ and $S_1Tyr_Z^{\bullet}$, respectively. The lifetime of $Tyr_Z^{\bullet}$ formed is a few minutes at cryogenic temperature, which is about 10^7 times longer than that at room temperature. These findings [23–27] provide a new way to investigate Tyr_Z in active PSII.

In this paper, possible interactions between Tyr_Z and substrate water were explored by studying the pH effect on Tyr_Z oxidation and $Tyr_Z^{\bullet}$ reduction at cryogenic temperature in active PSII

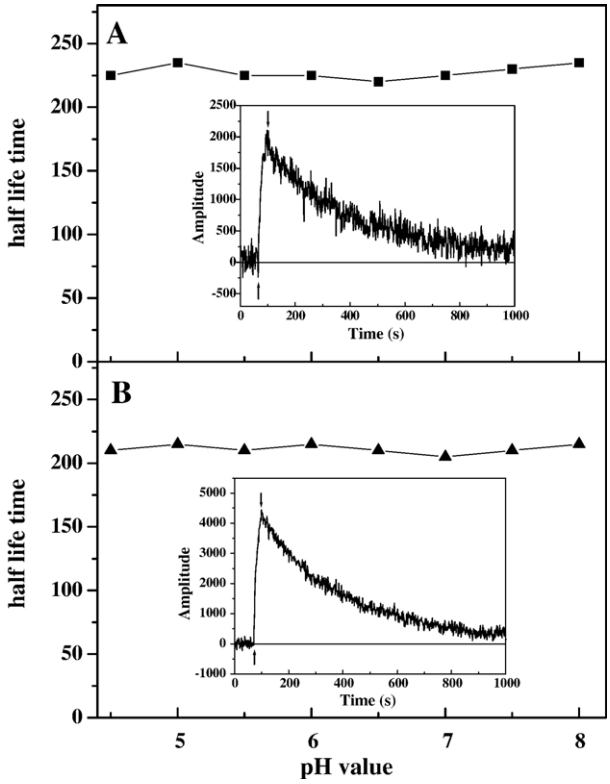

Fig. 2. pH dependence of the decay half-life time of $S_0Tyr_Z^{\bullet}$ (A) and $S_1Tyr_Z^{\bullet}$ (B) signal at dark at 5 K. Inset in A shows the induction and decay kinetics of the $S_0Tyr_Z^{\bullet}$ from the 3-flash sample recorded by monitoring the $S_0Tyr_Z^{\bullet}$ signal at 3280 G (see inset in Fig. 1A). Inset in B shows the induction and decay kinetic of the $S_1Tyr_Z^{\bullet}$ signal from the 0-flash sample recorded by monitoring the $S_1Tyr_Z^{\bullet}$ signal at 3300G (see inset in Fig. 1B). EPR conditions: conversion time, 1311 ms; time constant, 655 ms; sweep time, 1342 s; other settings are the same as Fig. 1. The arrows in the insets indicate when the lamp was turned on (↑) and turned off (↓).

with the method developed recently [23–27], as well as DFT calculations on model systems.

2. Materials and methods

PS II-enriched membranes were prepared from spinach as described in Ref. [28,29]. PSII membranes were dissolved in a medium containing 400 mM sucrose, 15 mM NaCl, 50 mM MES/NaOH (pH=6.0), and were frozen into liquid nitrogen and stored at −80 °C till to use.

PSII with Mn-cluster in different S-states was prepared as following: The samples were thawed and washed with a buffer containing 400 mM sucrose, 15 mM NaCl, 5 mM $MgCl_2$, 5 mM $CaCl_2$, 2 mM EDTA, and 0.5 mM MES/NaOH (pH 6.5). Then they were washed once with the same buffer without EDTA. The samples were finally resuspended in the same buffer without EDTA, and put into calibrated EPR tubes. The final concentration was about 2.5 mg Chl/ml. To synchronize all PSII in the $Tyr_D^{\bullet} S_1$ state, one pre-flash was given to the sample after 1 min incubation at room temperature and followed by 12–15 min dark adaptation at room temperature. External electron acceptor, PPBQ from a fresh 20 mM solution in DMSO was added to a final concentration of 1 mM. One minute after the addition of the external electron acceptor, the samples were exposed to 0 or 3 saturating laser flashes (7 ns, 532 nm, 550 mJ) at 1 Hz provided by an Nd:YAG laser (Spectra Physics) at room temperature. The pH of solution was adjusted by adding 15% (v/v) buffer solutions containing 400 mM sucrose, 15 mM NaCl, 5 mM $MgCl_2$, 5 mM $CaCl_2$ and 200 mM buffer at various pH immediately after flashing, and the sample solution was mixed by using a long needle with spiral shaped tip. The final buffer concentration was 30 mM. (Glutamic acid for pH 4.0–4.75, MES for pH 5.0–6.5, MOPS for pH 7.0–8.0, Gly–Gly for pH 8.25–9.0). Thirty seconds after laser flashes, the sample was frozen within 1-2 s, first in dry ice/ethanol, then cooled in liquid nitrogen.

Low temperature continuous wave EPR spectra and kinetics were recorded on a Bruker E300/E200 spectrometer equipped with an Oxford-900 liquid helium cryostat and ITC-503 temperature controller (Oxford Instruments Ltd.). A Bruker ST4102 standard cavity was used for all the measurements. Before EPR measurements, all samples were degassed with argon at 200 K. Illumination at liquid helium temperature was carried out directly in the EPR cavity as described in Ref. [24]. Spectrometer settings were given in the figure legends. After EPR measurements, the pH of each sample was measured at room temperature.

The calculation models were built up by simplifying Tyr and His with p-cresol and imidazole, respectively (see Fig. 3). The full geometric optimisation of the models in gas phase was performed by using (U)B3LYP/6-31G(D) method. The total energy of the systems were calculated at (U)B3LYP/6-311+G(1d, 1p) level and corrected by zero-point energies calculated with (U)B3LYP/6-31G(D) method. Similar method has been used to investigate the function and mechanism of Tyr_Z in PSII [30,31]. All calculations were carried out by using Gaussian 98 program [32].

3. Results and discussions

The EPR signals indicating oxidation of Tyr_Z were induced by continuous visible light illumination at 5 K [23–27]. The light

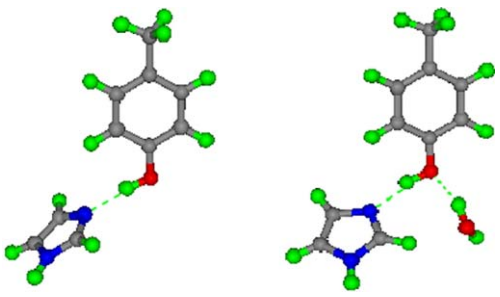

Fig. 3. Calculation models for Tyr–His (left) and Tyr–His–H_2O(right). (hydrogen in green, oxygen in red, nitrogen in blue). (For interpretation of the references to colour in this figure legend, the reader is referred to the web version of this article.)

Table 1
Energy comparison between Tyr–His and H_2O–Tyr–His models

	Tyr–His	Tyr–His–H_2O	Energy difference
HOMO energy (kcal/mol)	−124.93	−132.35	−7.42
Vertical ionization energy (kcal/mol)	169.05	174.79	5.74
Adiabatic ionization energy (kcal/mol)	153.61	153.92	0.31

induced $S_0Tyr_Z^{\bullet}$ and $S_1Tyr_Z^{\bullet}$ signals from 3-flash and 0-flash samples at pH 6.5, respectively, are shown in the inserts of Fig. 1A and B. Fig. 1A shows the pH effect on the formation of $S_0Tyr_Z^{\bullet}$ signals from 3-flash samples at pH range from 4 to 9. A bell-shaped pH-titration curve is obtained. The maximum amplitude is observed between pH 5 and 7, which is essentially unchanged over this pH range. However, the amplitude decreases at further lower or higher pH values. Two apparent p*K*s, 4.7±0.1 and 7.7±0.1, at low and high pH, respectively, were obtained from the curve. The pH effect on the formation of $S_1Tyr_Z^{\bullet}$ signal in 0-flash samples is shown in Fig. 1B. A bell shaped pH titration curve is obtained with the maximum amplitude around pH 6.0. The amplitudes decrease successively when the pH increases or decreases from 6.0. Two p*K*s, 4.9±0.1 and 7.7±0.1, at low and high pH range, respectively, were obtained. The pK_a values here (4.7–4.9 and 7.7) are close to those reported for pH effect on oxygen evolution and the multiline EPR signal of the Mn-cluster [33,34]. The pK_a for acidic pH region is similar to the value obtained in PSII sample isolated from thermophilic cyanobacterium (pK_a=4.6) [35], which was interpreted by titration of His190 in intact PSII. However, it was also possible due to release of the Ca from Mn-cluster as pointed out by the same authors [35,36]. Because the PSII reaction center loses the oxygen evolving activity at lower or higher pH, the observed pH-dependent part at low pH and high pH should be assigned to the inactive samples due to the inhibition at either donor side or acceptor side of PSII, rather than active PSII.

The above explanation is further supported by measuring the decay kinetics of above two visible light-induced EPR signals, as shown in Fig. 2. The decay kinetics of $S_0Tyr_Z^{\bullet}$ and $S_1Tyr_Z^{\bullet}$ signals are similar to our previous reports [23,24] (shown in the two insets in Fig. 2). Fig. 2A shows the decay lifetime ($\tau_{1/2}$) of the $S_0Tyr_Z^{\bullet}$ signals at 5K, which is 210±10 s at the whole pH range from 4.5 to 8.0. Similarly, lifetime ($\tau_{1/2}$) of the $S_1Tyr_Z^{\bullet}$ signals at 5 K remains as 225±10 s at the pH range from 4.5 to 8.0 (Fig. 2B). These results clearly indicate that the decay kinetics of the $S_1Tyr_Z^{\bullet}$ and $S_0Tyr_Z^{\bullet}$ signals are completely pH-independent at pH rang from 4.5 to 8.0.

It is worth mentioning that other states (e.g., S_2, S_3) in the samples do not give rise to comparable EPR signals under the present experimental conditions [23]. Therefore, contributions from these two states can be ruled out, this is not the case in reports using flash photolysis absorption spectroscopic measurement [37,38]. Because the formation and decay of $S_1Tyr_Z^{\bullet}$ and $S_0Tyr_Z^{\bullet}$ signals correspond to the Tyr_Z oxidation and $Tyr_Z^{\bullet}$ reduction, respectively [23–27], the present pH effect data indicate that both Tyr_Z oxidation and $Tyr_Z^{\bullet}$ reduction may be pH independent in active PSII samples in the S_0 and S_1 states. This behaviour is dramatically different to that of Tyr in solution and

the Tyr_Z in Mn- or Ca-depleted PSII samples, where both oxidation and reduction of Tyr are strongly pH dependent [9,10,20,39–41].

It is generally agreed that Tyr_Z radical formed after its oxidation is in its neutral state [9,10,38–40]. In Mn-depleted PSII, the reduced Tyr_Z is in its protonated form at physiological pH [9,10]. However, information about the protonation state of reduced Tyr_Z in active PSII is rather limited. It in principle can exist in two forms, deprotonated and protonated forms. In order to interpret the present pH dependence data, we consider both deprotonated and protonated forms. Firstly, if Tyr_Z was in its deprotonated form as proposed by Candeias et al. [42] and Haumann et al. [43], the oxidation of $TyrO^-$ (reaction (1)) should be pH-independent due to the lack of protons involved in this reaction.

$$TyrO^- \Leftrightarrow Tyr{-}O^{\cdot} + e^- \qquad \text{reaction 1}$$

$$TyrOH \Leftrightarrow Tyr{-}O^{\cdot} + H^+ + e^- \qquad \text{reaction 2}$$

This explanation seems fit our data well. However, we notice that the deprotonation of Tyr_Z normally requires a strong base ($pK_a > 10$) nearby, while the histidine (D1-His190, $pK_a \sim 6–7$) is the only amino acid residue around Tyr_Z in PSII [3,4]. Therefore, it is less likely to be the case. Secondly, if Tyr_Z was in its protonated form, the TyrOH oxidation should be dependent on its local pH (reaction (2)), which is obviously contradicted to the pH independent feature reported here. Alternatively, Tyr_Z is located at a hydrophobic environment, where bulk H_2O molecules and protons (H_3O^+) do not have access, thus the change of pH in bulk may have no effect on the local pH of Tyr_Z in active PSII. This rationalization is consistent with the recent suggestion of a low barrier hydrogen bond between Tyr_Z and $D1\text{-}His_{190}$ in active PSII [23], since most of the low barrier hydrogen bonds have been found in hydrophobic environments [44]. This suggestion is also consistent with the temperature dependence of $P_{680}^{+\cdot}$ reduction by Tyr_Z as reported by Renger et al. [45] They found that the activation energies for Tyr_Z oxidation was much lower in intact than in Mn-depleted PSII, and inferred that Tyr_Z was most "dry" and hydrophobic in intact PSII, but became enriched with water molecules after Mn-depletion [45]. One may argue that there could be a few substrate H_2O molecules even in the hydrophobic environment and that changing the pH in the bulk solution would have little effect on the Tyr_z and H_2O inside. If this were the case, we would expect a much slower exchange rate for the substrate H_2O. However, recent time-resolved mass spectroscopy studies [46] have reported a time constant of faster than $120s^{-1}$ for the substrate exchange rate in S_0 and S_1 states, which implies that if any substrate water molecule interacted with Tyr_Z, it should be able to exchange with bulk water in the mixing time in the experiment (see Materials and methods), and affect the oxidation and reduction behaviour of Tyr_Z. Therefore, it is likely that Tyr_Z is located in a hydrophobic environment and does not interact with substrate water in active PSII. This suggestion fits the proton-rocking model, in which Tyr_Z forms a strong hydrogen bond with adjacent His190, and the proton is located and shuttled between them [20,36,47–49]. This proton-rocking model is not expected to be pH-dependent and it is readily reconciled with the published very low kinetic H/D-isotope effect [36,47,50].

To further investigate if there was direct interaction between Tyr_Z and H_2O molecules in active PSII, a DFT theoretical study was carried out following procedures in previous reports [30,31]. The calculation models were simplified by substituting Tyr and His with p-cresol and imidazole, respectively (see Fig. 3). Interestingly, upon adding a H_2O molecule to this model (Fig. 3 right), the HOMO energy level was lowered by 7.42 kcal/mol, and the vertical ionization energy and the adiabatic ionization energy were increased by 5.74 kcal/mol and 0.31 kcal/mol, respectively (Table 1). These data clearly indicate that Tyr becomes more difficult to oxidize when a H_2O molecule interacts directly with it. Considering that Tyr_Z donates an electron to $P_{680}^{+\cdot}$ more efficiently in active PSII than in Mn-depleted PSII, it is reasonable to infer that there might be no water molecules interacting with Tyr_Z in active PSII. Therefore, in contrast to the situation in Mn-depleted PSII samples [9,10,22], Tyr_Z in active PSII is probably located in a hydrophobic environment, and no water molecules have interactions with it.

4. Conclusion

In summary, the maximum yield of Tyr_Z oxidation at cryogenic temperature in S_0 and S_1 states was observed at neutral range (pH 5–7) and it was pH independent in this pH range. The yield of Tyr_Z oxidation did however decrease in the acidic and alkaline pH regions, with two p*K*s, 4.7–4.9 and 7.7±0.1, respectively. The observed pH-dependencies at low pH and high pH are more likely to be due to inactive samples rather than active PSII. The reduction kinetics of $Tyr_Z^{\cdot}$ in the S_0 and S_1 states were pH independent in the pH range from 4.5 to 8. Therefore, the change of the pH in bulk solution has no effect on the Tyr_Z oxidation and $Tyr_Z^{\cdot}$ reduction at cryogenic temperature in the S_0 and S_1 states of the active PSII. It is reasonable to infer that Tyr_Z is probably located in a hydrophobic environment without substrate water molecule access in the S_0 and S_1 states of the active PSII. DFT calculations on model systems point to exclude also direct interaction between Tyr_Z and the substrate H_2O in functional PSII. These results challenge the previous postulation of direct interaction between Tyr_Z and the substrate water during water oxidation. Investigations on the higher oxidation states (e.g., S_2, S_3 states) are currently underway to explore whether Tyr_Z interacts with substrate water in these states. As it has been suggested [5,20,40,51,52] that the function of Tyr_Z could be different in S_2 and S_3 states with the S_0 and S_1 states, these studies will provide new insights on the function and mechanism of Tyr_Z in active PSII.

Acknowledgments

The author thanks Prof. A. W. Rutherford for discussion and encouragement. This work was supported by the DRI of the CEA Saclay, France, and the National Natural Science Foundation of China (No. 20403024 and 30570423).

References

[1] A. Zouni, H.T. Witt, J. Kern, P. Fromme, N. Krauss, W. Saenger, P. Orth, Crystal structure of photosystem II from *Synechococcus elongatus* at 3.8 Å resolution, Nature 409 (2001) 739–743.

[2] N. Kamiya, J.R. Shen, Crystal structure of oxygen-evolving photosystem II from *Thermosynechococcus vulcanus* at 3.7-Å resolution, Proc. Natl. Acad. Sci. U. S. A. 100 (2003) 98–103.

[3] K.N. Ferreira, T.M. Iverson, K. Maghlaoui, J. Barber, S. Iwata, Architecture of the photosynthetic oxygen-evolving center, Science 303 (2004) 1831–1838.

[4] B. Loll, J. Kern, W. Saenger, A. Zouni, J. Biesiadka, Towards complete cofactor arrangement in the 3.0 ? resolution structure of photosystem II, Nature 438 (2005) 1040–1044.

[5] G. Renger, Photosynthetic water oxidation to molecular oxygen: apparatus and mechanism, Biochim. Biophys. Acta 1503 (2001) 210–228.

[6] J.M. Peloquin, R.D. Britt, EPR/ENDOR characterization of the physical and electronic structure of the OEC Mn cluster, Biochim. Biophys. Acta 1503 (2001) 96–111.

[7] C. Goussias, A. Boussac, A.W. Rutherford, Photosystem II and photosynthetic oxidation of water: an overview, Philos. Trans. R. Soc. Lond., B 357 (2002) 1369–1381.

[8] J. Messinger, Evaluation of different mechanistic proposals for water oxidation in photosynthesis on the basis of Mn4OxCa structures for the catalytic site and spectroscopic data, Phys. Chem. Chem. Phys. 6 (2004) 4764–4771.

[9] R.J. Debus, Amino acid residues that modulate the properties of tyrosine YZ and the manganese cluster in the water oxidizing complex of photosystem II, Biochim. Biophys. Acta 1503 (2001) 164–186.

[10] B.A. Diner, Amino acid residues involved in the coordination and assembly of the manganese cluster of photosystem II. Proton-coupled electron transport of the redox-active tyrosines and its relationship to water oxidation, Biochim. Biophys. Acta 1503 (2001) 147–163.

[11] C.W. Hoganson, G.T. Babcock, A metalloradical mechanism for the generation of oxygen from water in photosynthesis, Science 277 (1997) 1953–1956.

[12] C. Tommos, G.T. Babcock, Oxygen production in nature: a light-driven metalloradical enzyme process, Acc. Chem. Res. 31 (1998) 18–25.

[13] C. Tommos, Electron, proton and hydrogen-atom transfers in photosynthetic water oxidation, Philos. Trans. R. Soc. Lond., B 357 (2002) 1383–1394.

[14] A. Boussac, J.L. Zimmermann, A.W. Rutherford, EPR signals from modified charge accumulation states of the oxygen-evolving enzyme in calcium-deficient photosystem II, Biochemistry 28 (1989) 8984–8989.

[15] M.L. Gilchrist, J.A. Ball, D.W. Randall, R.D. Britt, Proximity of the manganese cluster of photosystem II to the redox-active tyrosine YZ, Proc. Natl. Acad. Sci. U. S. A. 92 (1995) 9545–9549.

[16] H. Mino, A. Kawamori, Microenvironments of tyrosine D^+ and tyrosine Z^+ in photosystem II studied by proton matrix ENDOR, Biochim. Biophys. Acta 1185 (1994) 213–222.

[17] C. Tommos, X.S. Tang, K. Warncke, C.W. Hoganson, S. Styring, J. McCracken, B.A. Diner, G.T. Babcock, Spin-density distribution, conformation, and hydrogen bonding of the redox-active tyrosine Y_Z in photosystem II from multiple-electron magnetic-resonance spectroscopies: implications for photosynthetic oxygen evolution, J. Am. Chem. Soc. 117 (1995) 10325–10335.

[18] X.S. Tang, M. Zheng, D.A. Chisholm, G.C. Dismukes, B.A. Diner, Investigation of the differences in the local protein environments surrounding tyrosine radicals $YZ^\bullet$ and $YD^\bullet$ in photosystem II using wild-type and the D2-Tyr160Phe mutant of *Synechocystis* 6803, Biochemistry 35 (1996) 1475–1484.

[19] J. Yano, J. Kern, K.D. Irrgang, M.J. Latimer, U. Bergmann, P. Glatzel, Y. Pushkar, J. Biesiadka, B. Loll, K. Sauer, J. Messinger, A. Zouni, V.K. Yachandra, X-ray damage to the Mn_4Ca complex in single crystals of photosystem II: a case study for metalloprotein crystallography, Proc. Natl. Acad. Sci. U. S. A. 102 (2005) 12047–12052.

[20] W. Junge, M. Haumann, R. Ahlbrink, A. Mulkidjanian, J. Clausen, Electronstatics and proton transfer in photosynthetic water oxidation, Philos. Trans. R. Soc. Lond., B 357 (2002) 1407–1418.

[21] C. Tommos, G.T. Babcock, Proton and hydrogen currents in photosynthetic water oxidation, Biochim. Biophys. Acta 1458 (2002) 199–219.

[22] B.A. Diner, D.A. Force, D.W. Randall, R.D. Britt, Hydrogen bonding, solvent exchange, and coupled proton and electron transfer in the oxidation and reduction of redox-active tyrosine YZ in Mn-depleted core complexes of photosystem II, Biochemistry 37 (1998) 17931–17943.

[23] C. Zhang, S. Styring, Formation of split electron paramagnetic resonance signals in photosystem II suggests that tyrosineZ can be photooxidized at 5 K in the S_0 and S_1 states of the oxygen-evolving complex, Biochemistry 42 (2003) 8066–8076.

[24] C. Zhang, A. Boussac, A.W. Rutherford, Low-temperature electron transfer in photosystem II: a tyrosyl radical and semiquinone charge pair, Biochemistry 43 (2004) 13787–13795.

[25] J.H.A. Nugent, I.P. Muhiuddin, M.C.W. Evans, Electron transfer from the water oxidizing complex at cryogenic temperatures: the S_1 to S_2 step, Biochemistry 41 (2002) 4117–4126.

[26] J.H.A. Nugent, I.P. Muhiuddin, M.C.W. Evans, Effect of hydroxylamine on photosystem II: reinvestigation of electron paramagnetic resonance characteristics reveals possible S state intermediates, Biochemistry 42 (2003) 5500–5507.

[27] D. Koulougliotis, J.R. Shen, N. Ioannidis, V. Petrouleas, Near-IR irradiation of the S_2 state of the water oxidizing complex of photosystem II at liquid helium temperatures produces the metalloradical intermediate attributed to $S_1Y_Z^\bullet$, Biochemistry 42 (2003) 3045–3053.

[28] D.A. Berthold, G.T. Babcock, C.F. Yocum, A highly resolved, oxygen-evolving photosystem II preparation from spinach thylakoid membranes, FEBS Lett. 134 (1981) 231–234.

[29] K.A. Campbell, W. Gregor, D.P. Pham, J.M. Peloquin, R.J. Debus, R.D. Britt, The 23 and 17 kDa extrinsic proteins of photosystem II modulate the magnetic properties of the S1-state manganese cluster, Biochemistry 37 (1998) 5039–5045.

[30] M.R.A. Blomberg, P.E.M. Siegbahn, G.T. Babcock, Modeling electron transfer in biochemistry: a quantum chemistry study of charge separation in *Rhodobacter sphaeroids* and photosystem II, J. Am. Chem. Soc. 120 (1998) 8812–8824.

[31] F. Himo, P.E.M. Siegbahn, Quantum chemical studies of radical-containing enzymes, Chem. Rev. 103 (2003) 2421–2456.

[32] M.J. Frisch, G.W. Trucks, H.B. Schlegel, G.E. Scuseria, M.A. Robb, J.R. Cheeseman, V.G. Zakrzewski, J.A. Montgomery Jr., R.E. Stratmann, J.C. Burant, S. Dapprich, J.M. Millam, A.D. Daniels, K.N. Kudin, M.C. Strain, O. Farkas, J. Tomasi, V. Barone, M. Cossi, R. Cammi, B. Mennucci, C. Pomelli, C. Adamo, S. Clifford, J. Ochterski, G.A. Petersson, P.Y. Ayala, Q. Cui, K. Morokuma, D.K. Malick, A.D. Rabuck, K. Raghavachari, J.B. Foresman, J. Cioslowski, J.V. Ortiz, B.B. Stefanov, G. Liu, A. Liashenko, P. Piskorz, I. Komaromi, R. Gomperts, R.L. Martin, D.J. Fox, T. Keith, M.A. Al-Laham, C.Y. Peng, A. Nanayakkara, C. Gonzalez, M. Challacombe, P.M.W. Gill, B. Johnson, W. Chen, M.W. Wong, J.L. Andres, C. Gonzalez, M. Head-Gordon, E.S. Replogle, J.A. Pople, Gaussian 98 program, Gaussian, Inc., Pittsburgh PA, 1998.

[33] P. Geijer, S. Peterson, K.A. Åhrling, Z. Deák, S. Styring, Comparative studies of the S_0 and S_2 multiline electron paramagnetic resonance signals from the manganese cluster in Photosystem II, Biochim. Biophys. Acta 1503 (2001) 83–95.

[34] G. Bernát, F. Morvaridi, Y. Feyziyev, S. Styring, pH dependence of the four individual transitions in the catalytic S-cycle during photosynthetic oxygen evolution, Biochemistry 41 (2002) 5830–5843.

[35] P. Kühn, J. Pieper, O. Kaminskaya, H.J. Eckert, R.E. Lechner, V. Shuvalov, G. Renger, Reaction pattern of Photosystem II: oxidative water cleavage and protein flexibility, Photosynth. Res. 84 (2005) 317–323.

[36] G. Christen, A. Seeliger, G. Renger, $P680^{+\bullet}$ Reduction kinetics and redox transition probability of the water oxidizing complex as a function of pH and H/D isotope exchange in spinach thylakoids, Biochemistry 38 (1999) 6082–6092.

[37] E. Schlodder, B. Meyer, pH dependence of oxygen evolution and reduction kinetics of photooxidized chlorophyll aII (P-680) in photosystem II particles from *Synechococcus* sp, Biochim. Biophys. Acta 890 (1987) 23–31.

[38] B. Meyer, E. Schlodder, J.P. Dekker, H.T. Witt, O_2 evolution and Chl a_{II}^+ ($P\text{-}680^+$) nanosecond reduction kinetics in single flashes as a function of pH, Biochim. Biophys. Acta 974 (1989) 36–43.

[39] M. Sjödin, S. Styring, B. Åkermark, L. Sun, L. Hammarstrom, Proton-coupled electron transfer from tyrosine in a tyrosine–ruthenium–tris–

bipyridine complex: comparison with tyrosineZ oxidation in photosystem II, J. Am. Chem. Soc. 122 (2000) 3932–3936.
[40] F. Rappaport, J. Lavergne, Coupling of electron and proton transfer in the photosynthetic water oxidase, Biochim. Biophys. Acta 1503 (2001) 246–259.
[41] H. Kühne, G.W. Brudvig, Proton-coupled electron-transfer involving tyrosine Z in photosystem II, J. Phys. Chem., B 106 (2002) 8189–8196.
[42] L.P. Candeias, S. Turconi, J.H.A. Nugent, Tyrosine Y_Z and Y_D of photosystem II: comparison of optical spectra to those of tyrosine oxidised by pulsed radiolysis, Biochim. Biophys. Acta 1363 (1998) 1–5.
[43] M. Haumann, A. Mulkidjanian, W. Junge, Tyrosine-Z in oxygen-evolving photosystem II: a hydrogen-bonded tyrosinate, Biochemistry 38 (1999) 1258–1267.
[44] W.W. Cleland, P.A. Frey, J.A. Gerlt, The low barrier hydrogen bond in enzymatic catalysis, J. Biol. Chem. 273 (1998) 25529–25532.
[45] G. Renger, G. Christen, M. Karge, H.J. Eckert, K.D. Irrgang, Application of the Marcus theory for analysis of the temperature dependence of the reactions leading to photosynthetic water oxidation: result and implications, J. Biol. Inorg. Chem. 3 (1998) 360–366.
[46] W. Hillier, T. Wydrzynski, Substrate water interactions within the photosystem II oxygen evolving complex, Phys. Chem. Chem. Phys. 6 (2004) 4882–4889.
[47] R. Ahlbrink, M. Haumann, D. Cherepanov, O. Bögershausen, A. Mulkidjanian, W. Junge, Function of tyrosine Z in water oxidation by photosystem II: electrostatical promotor instead of hydrogen abstractor, Biochemistry 37 (1998) 1131–1142.
[48] J.H.A. Nugent, A.M. Rich, M.C.W. Evans, Photosynthetic water oxidation: towards a mechanism, Biochim. Biophs. Acta 1503 (2001) 138–146.
[49] C. Zhang, M. Fikret, S. Styring. His190 might directly bridge Y_z and Mn-cluster: Mechanistic consequences for water oxidation deduced from DFT calculation, The Proceeding of 12th International Congress on Photosynthesis, 18–23, August 2001, S13–011.
[50] M. Karge, K.D. Irrgang, S. Sellin, R. Feinäugle, B. Liu, H.J. Eckert, H.J. Eichler, G. Renger, Effects of hydrogen/deuterium exchange on photosynthetic water cleavage in PS II core complexes from spinach, FEBS Lett. 378 (1996) 140–144.
[51] M. Haumann, W. Junge, Photosynthetic water oxidation: a simplex-scheme of its partial reactions, Biochim. Biophys. Acta 1411 (1999) 86–91.
[52] J.S. Vrettos, J. Limburg, G.W. Brudvig, Mechanism of photosynthetic water oxidation: combining biophysical studies of photosystem II with inorganic model chemistry, Biochim. Biophys. Acta 1503 (2001) 229–245.